

ACRYLAMIDE INVERSE MINIEMULSION POLYMERIZATION: *IN SITU*, REAL-TIME MONITORING USING NIR SPECTROSCOPY

M. M. E. Colmán¹, D. L. Chicoma², R. Giudici², P. H. H. Araújo¹ and C. Sayer^{1*}

¹Depto. de Engenharia Química e Alimentos, Universidade Federal de Santa Catarina, 88040-900, Brasil.

*E-mail: csayer@enq.ufsc.br

*E-mail: magdalena@enq.ufsc.br; pedro@enq.ufsc.br

²Depto. de Engenharia Química, Escola Politécnica, Universidade de São Paulo,
Av. Prof. Luciano Gualberto, Travessa 3, No. 380, 5508-010, São Paulo - SP, Brasil.

E-mail: dennis@lscp.pqi.ep.usp.br; rgiudici@usp.br

(Submitted: June 28, 2013 ; Revised: March 31, 2014 ; Accepted: April 30, 2014)

Abstract - In this work, the ability of on-line NIR spectroscopy for the prediction of the evolution of monomer concentration, conversion and average particle diameter in acrylamide inverse miniemulsion polymerization was evaluated. The spectral ranges were chosen as those representing the decrease in concentration of monomer. An increase in the baseline shift indicated that the NIR spectra were affected by particle size. Multivariate partial least squares calibration models were developed to relate NIR spectra collected by the immersion probe with off-line conversion and polymer particle size data. The results showed good agreement between off-line data and values predicted by the NIR calibration models and these latter were also able to detect different types of operational disturbances. These results indicate that it is possible to monitor variables of interest during acrylamide inverse miniemulsion polymerizations.

Keywords: Inverse miniemulsion polymerization; Acrylamide; Monitoring; Spectroscopy; NIR.

INTRODUCTION

Hydrophilic polymers have numerous applications, as flocculants, adhesives and viscosity control agent for petroleum, chemicals for the paper industry and mining processes, that represent a market that amounts to about a billion dollars each year (Ullmann's, 2000 and Qi *et al.*, 2009). Polyacrylamide is one of those hydrophilic polymers and considerable research has been done to improve its viscosity building capacity by increasing its molecular weight (Hunkeler, 1990) and modifying the polymer chain with a few hydrophobic moieties to create intermolecular hydrophobic association (Feng *et al.*, 2005).

Acrylamide polymerization is characterized by a high ratio between propagation and termination rate

coefficients, resulting in polymers with high molecular weights, high viscosity, and high heat release rate, leading to poor mixing and heat transfer when operated on an industrial scale (Lovell *et al.*, 1997). The compartmentalization of the radicals in submicron-sized particles provides several advantages for emulsion and miniemulsion polymerization techniques compared to bulk, solution and suspension polymerizations, such as higher reaction rate and higher molecular weights. In addition, the resulting product is a dispersion of submicrometric polymer particles and there are fewer problems due to heat transfer or mixing during the polymerization since the viscosity of the continuous phase is low. Specifically in miniemulsion polymerizations, due to the droplet nucleation mechanism, polymerization kinetics do not de-

*To whom correspondence should be addressed

pend on monomer transport through the continuous phase because an initiator soluble in the dispersed phase (droplets/particles) can be used (Capek, 2010). However, the intended mechanism in the miniemulsion polymerization is the nucleation mechanism of the droplets, but in some cases homogeneous and micellar nucleation can happen (Ouyang *et al.*, 2011a). Nevertheless, while the number of works involving direct miniemulsion polymerization (oil in water) has increased dramatically since the pioneering work of Ugelstad *et al.* (1973) in which it was shown that submicrometric monomer droplets could be efficiently nucleated and thus serve as the main polymerization locus, few studies are reported in the literature related to inverse miniemulsion polymerization (water in oil) (Capek, 2010). The dispersed phase (submicrometric droplets) of inverse miniemulsion polymerization is composed of a polar monomer, water and a costabilizer (lipophobe) to minimize diffusional degradation, also known as Ostwald ripening. The continuous phase, in which the droplets are dispersed, also contains a nonionic surfactant to retard coalescence (Landfester, 2000). Since monomer droplets/particles are the main polymerization locus and due to their high superficial area, the initiator may either be soluble in the dispersed phase (Capek, 2003; Qi *et al.*, 2007; Kobitskaya *et al.*, 2010) or in the continuous phase (Qi *et al.*, 2007; Kobitskaya *et al.*, 2010; Romio *et al.*, 2013) or in both phases, as in the case of the redox initiation system used by Blagodatskikh *et al.* (2006).

Monitoring polymer properties during the reaction is important to eliminate or reduce variations in product quality or other failure during the process. For over 30 years the development of optical fibers has benefited from major advances which put near infrared spectroscopic techniques in an outstanding position to monitor processes (Wolfbeis and Weidgnas, 2006). Furthermore, this technique has the advantages of ease of handling, and rapid measurements, the ability to monitor simultaneously different polymer properties (Reis *et al.*, 2003, 2004a, b, c; Chicoma *et al.*, 2010), as well as the possibility of using a multiplexer system. Concerning this, monitoring by spectroscopic techniques is driven by the need to improve existing technology to reduce costs and increase process safety, maintain or improve product quality, and reduce the amount of residual volatile organic compounds, since conventional analytical methods are time-consuming and are not readily adapted for real time measurements (Bauer *et al.*, 2000). The NIR comprises the spectral region from $12,500\text{ cm}^{-1}$ to 4000 cm^{-1} and mainly contains vibrational overtones and combination bands (Patnaik *et*

al., 2004). The elaboration of multivariate calibration models is required to relate NIR spectra with properties of interest (Santos *et al.*, 2005; Reis *et al.*, 2005, 2007, Silva *et al.*, 2011), such as monomer concentration, conversion, and droplet/particle diameters throughout the reactions.

In the present work the feasibility of using NIR spectroscopy for online monitoring of changes in monomer concentration, conversion and average particle diameter of inverse acrylamide miniemulsion polymerizations conducted at different temperatures and with different types of surfactants and initiators (oil- or water soluble) was verified. Polymerization reactions carried out in the batch mode were used for the development and validation of NIR calibration models. Experimental techniques such as gravimetry and photon correlation spectroscopy were respectively used to determine off-line residual acrylamide concentrations and intensity average particle size diameters. Spectra were collected using a NIR immersion probe in the transreflectance mode.

EXPERIMENTAL

The continuous lipophilic phase of the inverse miniemulsion was prepared by dissolving the surfactant, polyglycerol polyricinoleate (PGPR) or SPAN 60, in cyclohexane. In sequence, the monomer, acrylamide (AAM), and the costabilizers, sodium chloride (NaCl) and polyvinylpyrrolidone (PVP), were dissolved in water to prepare the aqueous phase. Two types of initiators were used, the water-soluble potassium persulfate (KPS) or the oil soluble 2,2'-azo-bisobutyronitrile (AIBN). The former was dissolved in the aqueous solution, while the latter was dissolved in a small amount cyclohexane and added to the reaction medium after the miniemulsification. Both phases were mixed and magnetically stirred for 30 min, forming a coarse emulsion. When the aqueous phase initiator was used, this step was performed at $10\text{ }^{\circ}\text{C}$ to prevent the onset of the reaction during miniemulsification. A Ultra Turrax Digital T25 homogenizer (5 min at 20000 rpm in an ice-water bath) was used to prepare the miniemulsion. The inverse miniemulsion was then transferred to a 250 mL jacketed reactor with a magnetic stirring bar and stirred under a nitrogen stream to avoid inhibition of the polymerization process by the presence of oxygen. All polymerizations were carried out between $55\text{ }^{\circ}\text{C}$ and $60\text{ }^{\circ}\text{C}$ (see Table 2). Figure 1 represents the experimental unit. The reactor is equipped with a magnetic stirrer, reflux condenser, sampling valve, nitrogen injection system, NIR immersion probe, and thermometer.

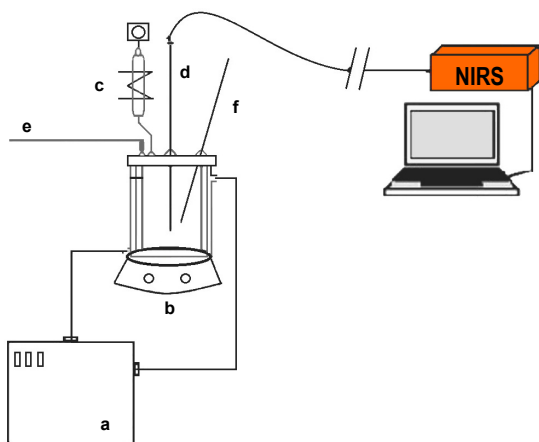


Figure 1: Scheme of the experimental setup: a - Thermostatic bath; b - Magnetic stirrer; c - Condenser; d - NIR probe; e - Nitrogen Stream; f - Thermometer.

Table 1 shows the recipe of the acrylamide inverse miniemulsion polymerizations. The differences among the reactions, initiator type and concentration, surfactant type and reaction temperature are shown in Table 2.

Table 1: Recipe used in the acrylamide inverse miniemulsion polymerizations.

Phase	Reagents (g)	Mass (g)
Dispersed	Water	15.0
	Acrylamide	11.2
	NaCl ^a	2.920
	PVP	0.94
	KPS	variable
Continuous	Cyclohexane	101.2
	PGPR or SPAN 60	6.02
	AIBN	variable

Table 2: Characteristics of inverse acrylamide miniemulsion polymerizations.

Run	Initiator		Surfactant		T (°C)
	KPS (%) ^a	AIBN (%) ^a	PGPR	Span 60	
M 1	2	---	X	---	63
M 2	2	---	X	---	60
M 3	1	---	X	---	65
M 4	2	---	X	---	65
M 5	2	---	X	---	55
M 6 ^b	2	---	X	---	55
M 7 ^c	1	---	---	X	60
M 8 ^d	1	---	---	X	60
M 9	---	3	X	---	60

^a wt% related to the mass of monomer

^b increase of reaction temperature to 65 °C after 180 min of reaction

^c without PVP

^d addition of 50 wt% of the reaction medium after 70 min of reaction

Latex characterization: samples were collected during the polymerization process to determine conversion and average particle diameter.

Conversion was determined by gravimetry based on the following procedure: samples were collected from the reactor and precipitated in an excess of chilled acetone containing 0.1 wt% of hydroquinone, and then separated by centrifugation. This procedure was repeated twice without hydroquinone to remove the non-polymeric solids. The precipitate was dried at 60 °C to remove residual acetone, cyclohexane and water. The conversion was calculated as the ratio between the mass of dry polymer and the amount of monomer that the sample taken from the reactor should contain if no reaction occurred. When PGPR, a surfactant with double bonds, was used, the procedure described by Hunkeler (1990) was followed to calculate conversion.

The intensity average particle diameter was measured by dynamic light scattering technique (DLS, Beckmann Coulter N4 Plus) diluting the samples in cyclohexane.

Online Monitoring

NIR spectra were collected online with an IFS 28/N Bruker spectrometer, equipped with a quartz beam splitter, using a probe (Hellma 661.622 NIR, with a transfection system and overall light path equal to 2 mm) immersed into the reaction medium. Spectral acquisition and processing were developed using the OPUS software package. Gravimetric (conversion and monomer concentration) and DLS (intensity average particle diameter) data were used as reference data in the multivariate partial least squares (PLS) calibration models.

RESULTS AND DISCUSSION

NIR Model of Acrylamide Concentration

To improve the quality of the calibration models, spectral pre-treatment techniques were applied. The second derivative with 25 points (smoothing) using the Savitzky–Golay method was chosen as the spectral pre-treatment technique due to its good results for this type of heterogeneous system (Vieira *et al.*, 2002; Chicoma, 2009). The Savitzky–Golay method is based on the polynomial fitting of spectra using partial least square regression, allowing data differentiation and smoothing. The calibration set of reactions, composed of polymerizations M 1, M 2 and M 3 in Table 2, was chosen to cover a wide range of conversion values.

Three different spectral regions were evaluated for the prediction of residual monomer concentration (Figure 2). Two of these regions correspond to those attributed to the decrease of the residual acrylamide concentration (4250 cm^{-1} - 4500 cm^{-1} and 5855 cm^{-1} - 6250 cm^{-1}) and the last involved the entire spectral region (4250 cm^{-1} - 12500 cm^{-1}). The best internal cross-validation results in terms of coefficient of determination ($R^2 = 0.994$) and root mean square error of cross validation (RMSECV) were obtained for the first overtone region (5855 - 6250 cm^{-1}) with seven principal components. Furthermore, it is important to note that a larger number of principal components may lead to an overfitting, incorporating noise into the calibration information.

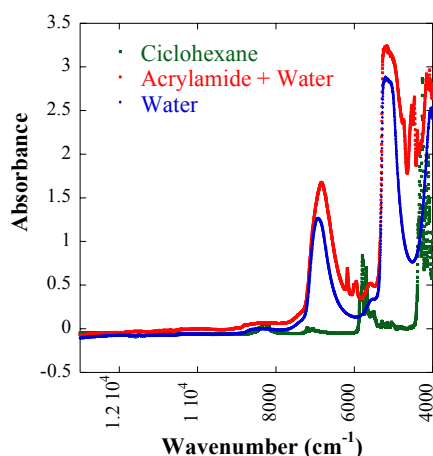


Figure 2: NIR spectra of the main components of acrylamide inverse miniemulsion polymerizations.

Estimation of Acrylamide Concentration and Conversion in Inverse Miniemulsion Polymerizations

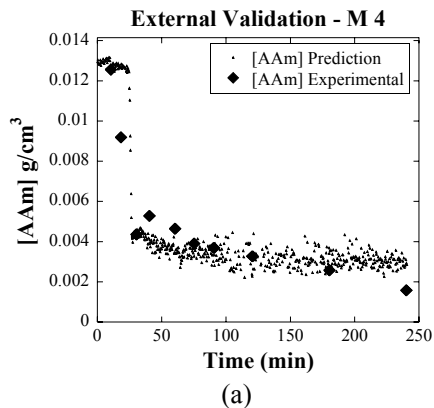
Figure 3 compares NIR and gravimetric results for the residual acrylamide concentration and conversion for inverse miniemulsion polymerizations that were not used in the calibration model. All reactions conducted with the aqueous phase initiator KPS, added to the dispersed phase prior to the miniemulsification procedure, show an initial conversion around 17%, followed by an induction period during the first minutes of reaction due to the presence of traces of oxygen (polymerization inhibitor). The induction period occurred for all reactions (with KPS and AIBN) since oxygen enters the reaction medium during the emulsification and homogenization (with Ultra Turrax) steps. The eventual presence of other impurities may also contribute to this induction period (Capek, 2010; Qi 2007, Ouyang *et al.*, 2011b). Though, initial induction periods are usually not desired, their presence does not hamper the purpose

of this work, which is to evaluate the ability of NIR spectroscopy to keep track of inverse acrylamide miniemulsion polymerizations despite the presence of disturbances. On the contrary, the ability to predict correctly the end of the induction period is a desired feature of process monitoring. After this initial induction period, reaction rate was very high due to the high propagation coefficient value of acrylamide, $k_p = 4.3 \times 10^4\text{ L}\cdot\text{mol}^{-1}\cdot\text{s}^{-1}$ at $60\text{ }^\circ\text{C}$ (Qi, 2009) until a limiting conversion between 70 and 80%, depending on the formulation, was reached.

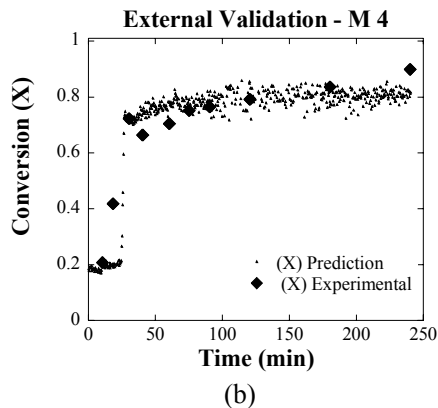
It can be observed in Figure 3 that the NIR model was able to describe correctly the trends of these reactions, including the initial induction period followed by a high reaction rate and the limiting conversion. However, some slight deviations can be observed, as in Reaction M 6 (Figure 3 (e) and (f)). In this experiment a disturbance, a temperature increase in the last hour of reaction, was applied to the system and the model was able to detect this operational disturbance. The trend of reaction M 7, carried out with the surfactant Span 60 and without PVP, and of reaction M 9, with the oil-soluble initiator AIBN, was described correctly by the calibration model based on reactions with KPS as initiator and PGPR as surfactant, but the NIR model results were noisier than in the other reactions. The higher noise in the NIR predictions of reactions M 7 and M 9 can be attributed to the interference of the different initiator and surfactant, respectively, used in these reactions. Finally, Figures 3 (i) and (j) show the results of reaction M 8 during which, after 70 min of reaction, 50 wt% of the total mass of the reaction medium was fed. Again, in this case the model was able to detect correctly the disturbance.

NIR Model for the Average Particle Diameter

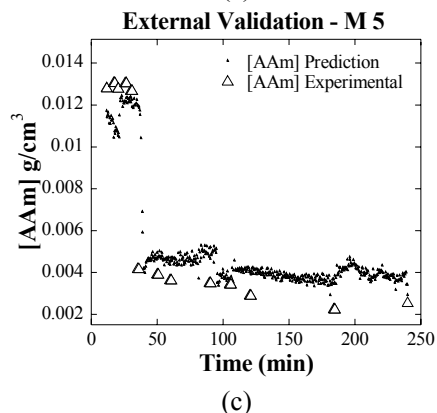
The reaction set for the calibration model of the average particle diameter was selected to cover a wide range of diameters (165 nm to 250 nm), and thus included reactions carried out with both types of surfactants, PGPR (M 1 and M 4) and Span 60 (M 7 and M 8). In addition, the spectral region between 9500 cm^{-1} and 12500 cm^{-1} was used for the average particle diameter model, because in this region the absorbance of the monomer is minimal and the effect of light scattering by the polymer particles is much more intense compared to other spectral regions where absorbance is predominant (Chicoma *et al.*, 2011). The first derivative with 17 point smoothing with normalization vector was used as the spectral pre-processing method. Based on cross-validation as internal validation, a PLS model with three principal components with $R^2 = 0.76$ and $\text{RMSECV} = 14.4\text{ nm}$ was chosen.



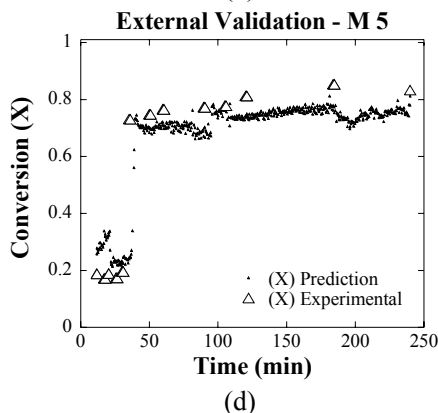
(a)



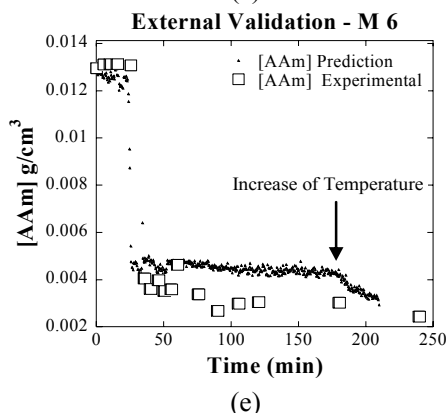
(b)



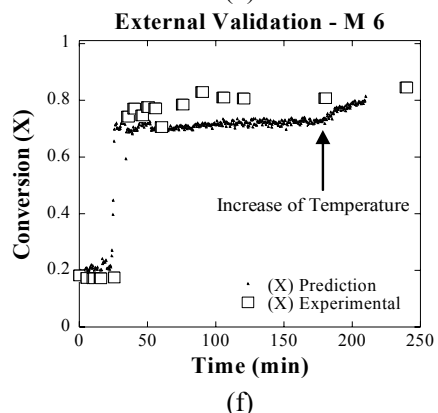
(c)



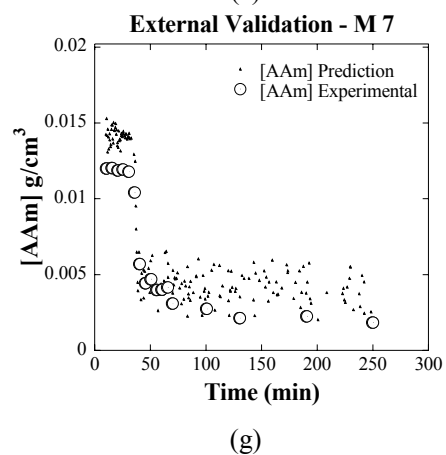
(d)



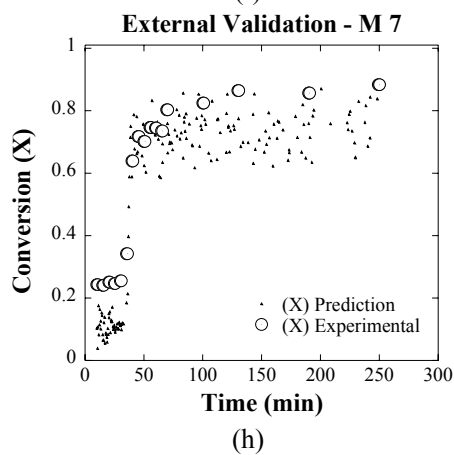
(e)



(f)



(g)



(h)

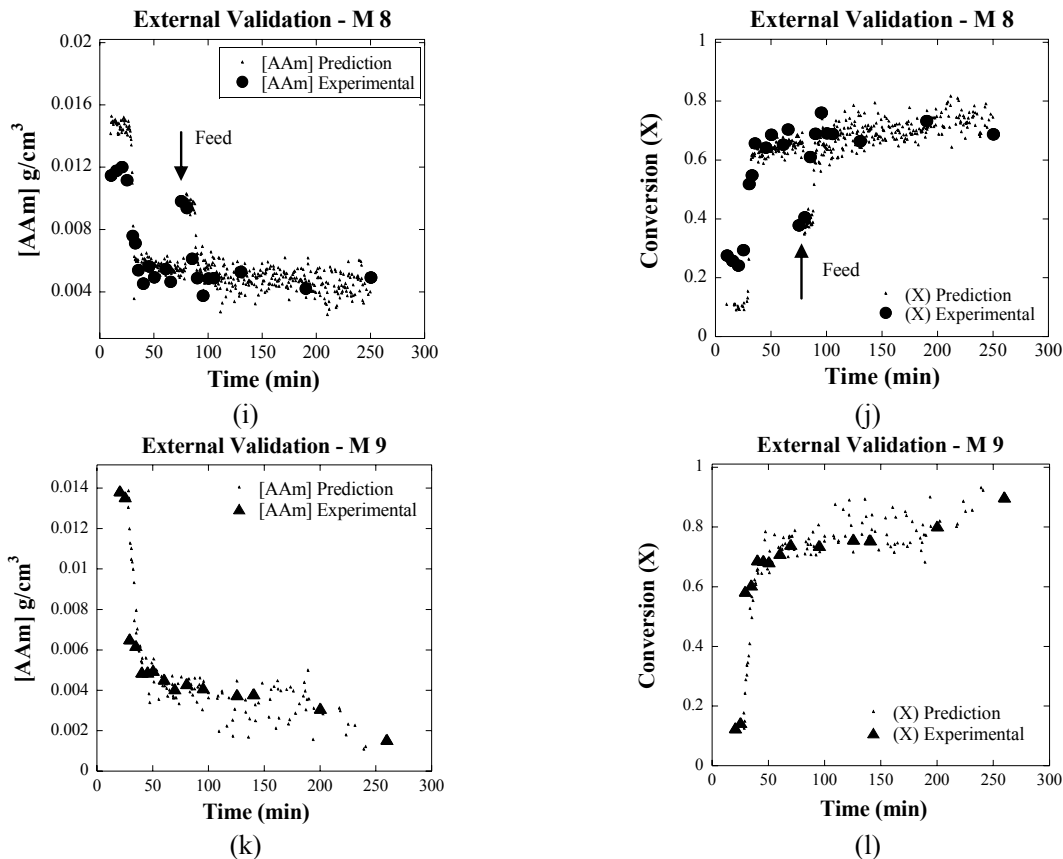


Figure 3: External validation of the NIR calibration model for the concentration of acrylamide (a), (c), (e), (g), (i), (k) and conversion (b), (d), (f), (h), (j), (l) during acrylamide inverse miniemulsion polymerizations.

Estimation of Particle Diameter in Inverse Acrylamide Miniemulsion Polymerizations

The external validation of the NIR model developed for the average particle diameter in acrylamide inverse miniemulsion polymerization is shown in Figure 4. The NIR model estimations agreed satisfactorily with D_p data determined offline by DLS, predicting correctly the timing of the abrupt particle size decrease observed for these reactions at around 30 min. The timing of this particle size decrease also agrees with the sharp increase in reaction rate (Fig. 2), indicating that possibly another particle nucleation mechanism besides the desired droplet nucleation is also active at this point.

Ouyang *et al.* (2011a) observed a large polydispersity of particles of poly(sodium acrylate) with acrylamide and poly(acrylamide) extended with acrylic acid. These authors indicated that the polydispersity was due to the phenomenon of Oswald ripening in which the smaller droplets with higher solubility diffuse to the larger monomer droplets. How-

ever, the surfactant barrier difficults the diffusion to the larger particles, but it does not disappear. Another important factor is the low solubility of acrylamide in cyclohexane. The same authors indicated that oligoradicals of acrylamide in the continuous phase can be quickly captured by micelles containing monomer, forming new particles by micellar nucleation.

While the NIR model was able to detect correctly the timing of this particle size decrease, it underestimated its magnitude as observed in the small deviations between NIR and DLS D_p values after 30 min of reaction. During the course of reactions M 2 and M 3, for which the particle size increased from 180 nm to 200 nm after 50 min of reaction, indicating particle coalescence, several smaller discontinuities may be observed in the D_p values predicted by the NIR model, in addition to the initial abrupt decrease also observed in the DLS data. As reported by Reis *et al.* (2004) for the styrene/butyl acrylate emulsion copolymerization reactions, particle coalescence might be the reason for the deviations in the particle size monitoring. When polymer particle aggregates are

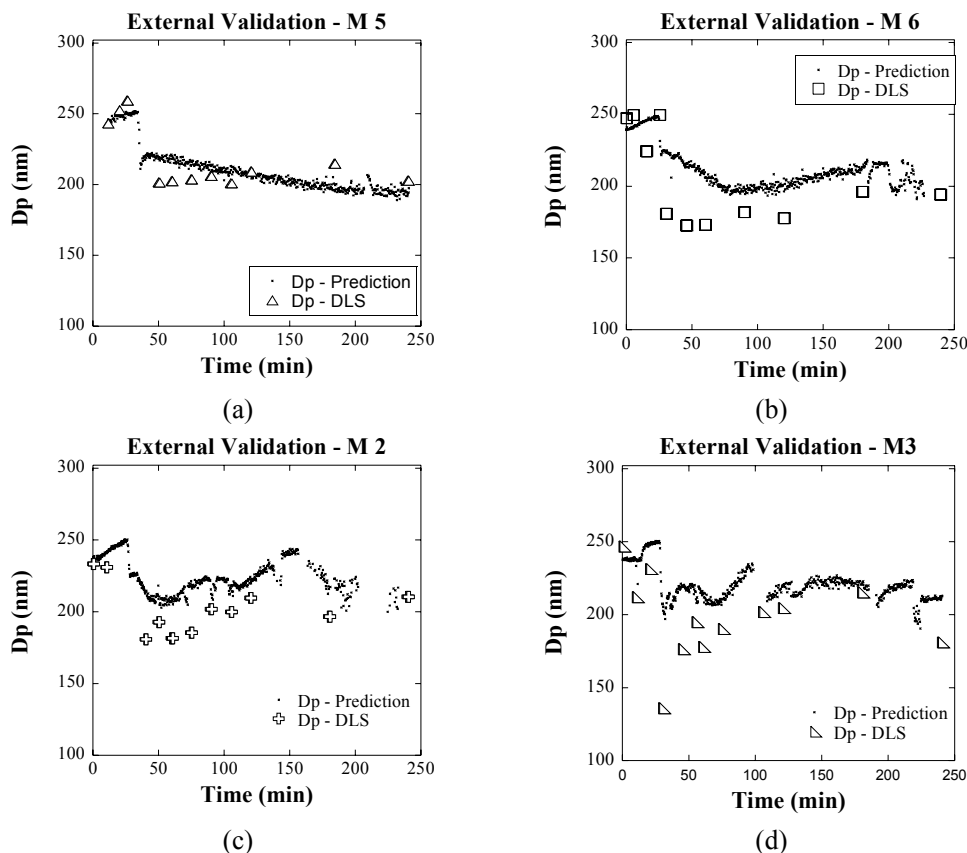


Figure 4: External validation of the NIR calibration model for the average particle diameter during acrylamide polymerizations of an inverse miniemulsion.

formed during emulsion/miniemulsion polymerizations, these might get stuck in the optical path of the NIR immersion probe, leading to deviations in the estimations of Dp until these aggregates are released and NIR estimations return to the correct values. This interference of the formation of aggregates in the NIR spectra, and thus in the estimation of Dp, may be used advantageously for the early detection of the formation of these aggregates during the process.

CONCLUSIONS

The use of NIR spectroscopy for monitoring acrylamide inverse miniemulsion polymerization was discussed in this work. Results showed the feasibility of on-line monitoring of conversion and average particle size in these inverse miniemulsion polymerization reactions using NIR spectroscopy. Using a 25-point second derivative with smoothing for spectral pretreatment, it was possible to develop a partial least squares calibration model for acrylamide concentration with a high determination coefficient.

External validation of acrylamide concentration and conversion predictions based on on-line NIR spectra showed a good agreement with off-line gravimetric data, keeping track of reaction trends such as the initial induction period, followed by a very sharp increase of reaction rate. Furthermore, NIR spectroscopy was able to detect disturbances such as additional reactant feeding and reaction temperature increase, allowing the possibility of acting on the system. The sensitivity of NIR spectroscopy toward the evolution of the average polymer particle diameter under different operational conditions of inverse miniemulsion polymerization reactions was evaluated with the online NIR probe. The changes of the particle diameter were detected successfully, also the estimation of complex phenomena like particle nucleation and coalescence.

ACKNOWLEDGMENT

The authors thank the financial support from CAPES (Coordenação de Aperfeiçoamento de Pessoal

de Nível Superior), CNPq (Conselho Nacional de Desenvolvimento Científico e Tecnológico) and FAPESP (Fundação de Amparo à Pesquisa do Estado de São Paulo).

REFERENCES

- Blagodatskikh, I., Tikhonov, V., Ivanova, E., Landfester, K., Khokhlov, A., New approach to the synthesis of polyacrylamide in miniemulsified systems. *Macromol. Rapid Commun.*, 27, p. 1900-1905 (2006).
- Bauer, C., Amram, B., Agnely, M., Charmot, D., Sawatzki, J., Dupuy, N., Huvenne, J. P., On-line monitoring of a latex emulsion polymerization by fiber-optic FT-Raman spectroscopy. Part I: calibration. *Appl. Spectrosc.*, 54, p. 528-535 (2000).
- Capek, I., The inverse mini-emulsion polymerization of acrylamide. *Design. Monom. Polym.*, 6, p. 399-409 (2003).
- Capek, I., On the inverse miniemulsion copolymerization and terpolymerization of acrylamide, N, N'-methylenebis (acrylamide) and methacrylic acid. *Central Europ. J. Chem.*, 3, p. 291-304 (2003).
- Capek, I., On inverse miniemulsion polymerization of conventional water – soluble monomers. *Adv. Colloid. Interf. Sci.*, 156, p. 35-61 (2010).
- Chicoma, D. L., Monitoramento em linha de reações de copolimerização em emulsão de acetato de vinila e acrilato de butila em um reator contínuo pulsado de pratos perfurados usando espectroscopia NIR. 2009. p. 233, Tese de Doutorado. Engenharia Química, Universidade de São Paulo, São Paulo (2009). (In Portuguese).
- Chicoma, D., Carranza, V., Sayer, C., Giudici, R., In line monitoring of VAc-BuA emulsion polymerization reaction in a continuous pulsed sieve plate reactor using NIR spectroscopy. *Macromol. Symp.*, 289, p. 140-148 (2010).
- Chicoma, D., Sayer, C., Giudici, R., In-line monitoring of particle size during emulsion polymerization under different operational conditions using NIR spectroscopy. *Macromol. React. Eng.*, 5, p. 150-162 (2011).
- Feng, Y., Billon, L., Grassl, B., Bastiat, G., Borisov, O., François, J., Hydrophobically associating polyacrylamides and their partially hydrolyzed derivatives prepared by post-modification. 2. Properties of non-hydrolyzed polymers in pure water and brine. *Polymer*, 46, p. 9283-9295 (2005).
- Hunkeler, D. J., Acrylic water soluble polymers. PhD. Thesis, Chemical Engineering, Mc Master University, Canada (1990).
- Kobitskaya, E., Ekinici, D., Manzke, A., Plettl, A., Wiedwald, U., Ziemann, P., Biskupek, J., Kaiser, U., Ziener, U., Landfester, K., Narrowly size distributed zinc-containing poly(acrylamide) latexes via inverse miniemulsion polymerization. *Macromolecules*, 43, p. 3294-3305 (2010).
- Landfester, K., Willert, M., Antonietti, M., Preparation of polymer particles in nonaqueous direct and inverse miniemulsions. *Macromolecules*, 33, p. 2370-2376 (2000).
- Lovell, P. A., El-Asser, M. S., Emulsion Polymerization and Emulsion Polymers. Chichester: J. Wiley (1997).
- Ouyang, L., Wang, L., Schork, F. J., Raft Inverse miniemulsion polymerization of acrylic acid and sodium acrylate. *Macromol. React. Eng.*, 5, p. 163-169 (2011a).
- Ouyang, L., Wang, L., Schork, F. J., Synthesis and nucleation mechanism of inverse emulsion polymerization of acrylamide by RAFT polymerization: A comparative study. *Polymer*, 52, p. 63-67 (2011b).
- Patnaik Pradyot, Dean's Analytical Chemistry Handbook. 2nd Edition, McGraw-Hill, p. 1143 (2004).
- Qi, G., Jones C. W., Schork, F. J., RAFT inverse miniemulsion polymerization of acrylamide. *Macromol. Rapid Commun.*, 28, p. 1010-1016 (2007).
- Qi, G., Eleazer, B., Jones, C. W., Schork, F. J., Mechanistic aspects of sterically stabilized controlled radical inverse miniemulsion polymerization. *Macromolecules*, 42, p. 3906-3916 (2009).
- Reis, M. M., Araújo, P. H. H., Sayer, C., Giudici, R., Correlation between polymer particle size and in-situ NIR spectra. *Macromolecular Rapid Communications*, 24(10), p. 620-624 (2003).
- Reis, M. M., Araújo, P. H. H., Sayer, C., Giudici, R., Comparing NIR Infrared and Raman spectroscopy for on-line monitoring of emulsion copolymerization reactions. *Macromol. Symp.*, 206, p. 165-178 (2004a).
- Reis, M. M., Araújo, P. H. H., Sayer, C., Giudici, R., In situ near-infrared spectroscopy for simultaneous monitoring of multiple process variables in emulsion copolymerization. *Ind. Eng. Chem. Res.* 43, p. 7243-7250 (2004b).
- Reis, M. M., Araújo, P. H. H., Sayer, C., Giudici, R., Development of calibration models for estimation of monomer concentration by Raman spectroscopy during emulsion polymerization: facing the medium heterogeneity. *Journal of Applied Polymer Science*, 93(3), p. 1136-1150 (2004c).
- Reis, M. M., Uliana, M., Sayer, C., Araújo, P. H. H., Giudici, R., Monitoring emulsion homopolymeri-

- zation reactions using FT-RAMAN spectroscopy. *Braz. J. Chem. Eng.*, 22, p. 61-74 (2005).
- Reis, M. M., Araújo, P. H. H., Sayer, C., Giudici, R., Spectroscopic on-line monitoring for dispersed medium reactions: Chemometric Challenges, *Analytica Chimica Acta*, 595(1-2), 257-265 (2007).
- Romio, A. P., Rodrigues, H. H., Peres, A., da Cas Viegas, A., Kobitskaya, E., Ziener, U., Landfester, K., Sayer, C., Araújo, P. H. H., Encapsulation of magnetic nickel nanoparticles via inverse miniemulsion polymerization. *J. Appl. Polym. Sci.*, p. 1426- 1433 (2013).
- Santos, A. F., Silva, F. M., Lenzi, M. K., Pinto, J. C., Monitoring and control of polymerization reactors using NIR spectroscopy. *Polymer-Plastics Technology and Engineering*, 44:1, 1-61 (2005)
- Silva, W. K., Chicoma, D., Giudici, R., In-situ real-time monitoring of particle size, polymer and monomer contents in emulsion polymerization of methyl methacrylate by near infrared spectroscopy. *Polymer Engineering and Science*, 51, 2024-2034 (2011).
- Ugelstad, J., El-Aasser, M. S., Vanderhoff, J. W. J., Emulsion polymerization: Initiation of polymerization in monomer droplets. *J. Polym. Sci., Polym. Lett.*, 11(8), p. 503-513 (1973).
- Ullman's Encyclopedia of Industrial Chemistry, Sixth Edition, Wiley-VCH, p. 8190 (2000).
- Vieira, R. A. M., Sayer, C., Lima, E. L., Pinto, J. C., In-line and in situ monitoring of semi-batch emulsion copolymerizations using near-infrared spectroscopy. *J. Appl. Polym. Sci.*, 84, p. 2670-2682 (2002).
- Wolfbeis, O. S., Weidgans, B. M., Fiber Optic Chemical Sensors and Biosensor: A view Back. In: Baldini, F. Chester, A. N., Homola, J., Martellucci, S., *Optical Chemical Sensors*. p. 17-44 (2004).